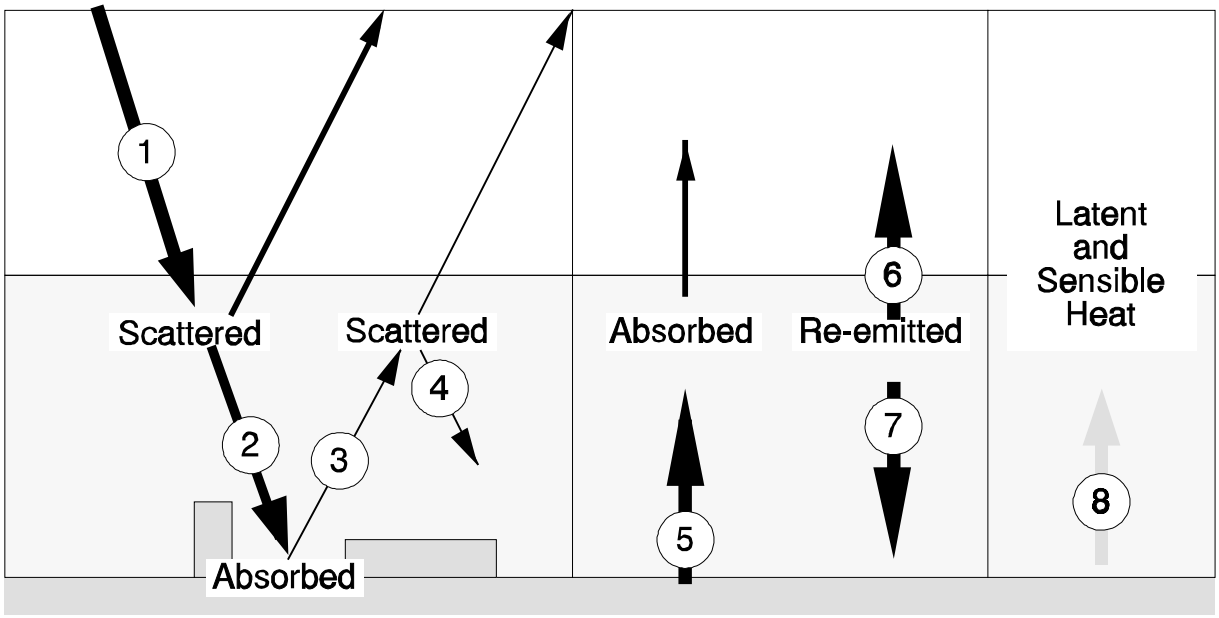

Figure 3-7. Surface radiation budget for short- and long-wave radiation. The surface radiation budget is driven by the input of short-wave radiation (1). This direct input is reduced by scatter (2) and absorption passing through the atmosphere. The amount that remains can be absorbed or reflected at the surface. The reflected light (3) also can be scattered back to the surface (4). The short-wave energy absorbed at the surface will ultimately be emitted back to the atmosphere as long-wave radiation (5). The atmosphere absorbs much of this radiation and radiates it back to the surface (7) and out to space (6). This energy cycle is completed as some of the absorbed energy is transmitted to the atmosphere as sensible and latent heat (8).

3.3.1.2 Planetary Boundary Layer

The concentration of an air pollutant depends significantly on the degree of mixing that occurs between the time a pollutant or its precursors are emitted and the arrival of the pollutant at the receptor. Atmospheric mixing is the result of either mechanical turbulence, often associated with wind shear, or thermal turbulence associated with vertical redistribution of heat energy. The potential for thermal turbulence can be characterized by atmospheric stability. The more stable the air layer, the more work is required to move air vertically.

As air is moved vertically through the atmosphere, as might happen in a convective thermal, its temperature will decrease with height as the result of adiabatic expansion. It is the comparison of how the temperature *should* change with height in the absence of external heating or cooling against the *actual* temperature change with height that is a measure of atmospheric stability. Those layers of the atmosphere where temperature increases with height (inversion layers) are the most stable as air, cooling as it rises, becomes denser than its new warmer environment. In an atmospheric layer with relatively low turbulence, pollutants do not redistribute vertically as rapidly as they do in an unstable layer.

Also, because a stable layer has a relatively low rate of mixing, pollutants in a lower layer will not mix through it to higher altitudes.

The stability of the atmosphere is often measured through computation of potential temperature as

$$\theta = \left(\frac{P}{P_o} \right)^{-R/c_p}, \tag{3-79}$$

where θ is the virtual potential temperature, P is the pressure of the air parcel, P_o is the reference pressure to which the air parcel will be moved (usually 1,000 mb), R is the gas law constant, and c_p is the specific heat of air at constant pressure. The faster θ increases with height, the less the potential for mixing.

A stable layer can also act as a trap for air pollutants lying beneath it. Hence, an elevated inversion is often referred to as a "trapping" inversion. On the other hand, if pollutants are emitted into a stable layer aloft, such as might occur from an elevated stack, the lack of turbulence will keep the effluents from reaching the ground while the inversion persists.

Traditionally, atmospheric mixing has been treated through use of a *mixing height*, which is defined as the base of an elevated inversion layer. In this model, the O_3 precursors are mixed uniformly through the layer below the mixing height. As this layer grows, it both entrains remnant O_3 from previous days and redistributes fresh emissions aloft. The vertical mixing profile through the lower layers of the atmosphere is assumed to follow a typical and predictable cycle on a generally clear day. In such a situation, a nocturnal surface inversion would be expected to form during the night as $L\uparrow$ exceeds $L\downarrow$. This surface layer inversion persists until surface heating becomes significant, probably 2 or 3 h after sunrise. Pollutants initially trapped in the surface inversion may cause relatively high, local concentrations, but these concentrations will decrease rapidly when the surface inversion is broken by surface heating. The boundary formed between the rising, cooling air of the growing mixing layer and that of the existing PBL is often sharp and can be observed as an elevated temperature inversion.

Elevated temperature inversions, when the base is above the ground, are also common occurrences (Hosler, 1961; Holzworth, 1964, 1972). This condition can form simply as the result of rapid vertical mixing from below, but is exacerbated in regions of subsiding air when the sinking air warms to a point at which it is warmer than the rising and cooling underlying air. Because these circumstances are associated with specific synoptic conditions, they are less frequent than the ubiquitous nighttime radiation inversion. An elevated inversion is, nevertheless, a very significant air pollution feature, because it may persist throughout the day and, thus, restrict vertical mixing.

When compared to a source near the surface and the effects of a radiation (surface) inversion, the pollutant dispersion pattern is quite different for an elevated source plume trapped in a layer near the base of an elevated inversion. This plume will not be in contact with the ground surface in the early morning hours because there is no mixing through the surface radiation inversion. Thus, the elevated plume will not affect surface pollutant concentrations until the mixing processes become strong enough to reach the altitude of the plume. At that time, the plume may be mixed downward quite rapidly in a process called

fumigation. During fumigation, surface O_3 concentrations will increase if the morning O_3 concentration is higher aloft than at the ground and if insufficient scavenging by NO occurs at ground-level. In fact, the rapid rise in O_3 concentrations in the morning hours is often the result of vertical (downward) transport from an elevated reservoir of O_3. After this initial increase, surface concentrations can continue to increase as a result of photochemistry or transport of O_3-rich air to the receptor.

When surface heating decreases in the late afternoon and early evening, the surface inversion will form again under most conditions. The fate of the elevated inversion is less clear, however. Although O_3 and its precursors have been mixed vertically, the reduction of turbulence and mixing at the end of the daylight hours leaves O_3 in a remnant layer that is often without a well-defined thermodynamic demarcation. This layer is then transported through the night, often to regions far removed from pollution sources, where its pollutants can influence concentrations at remote locations the next morning, as mixing entrains the elevated remnant layer. This overnight transport can be aided by the development of a nocturnal jet that forms many nights at the top of the surface inversion layer.

Geography can have a significant impact on the dispersion of pollutants (such as along the coast of an ocean or one of the Great Lakes). Near the coast or shore, the temperatures of land and water masses can be different, as can the temperature of the air above these land and water masses. When the water is warmer than the land, there is a tendency toward reduction in the frequency of surface inversion conditions inland over a relatively narrow coastal strip (Hosler, 1961). This in turn tends to increase pollutant dispersion in such areas. The opposite condition also occurs if the water is cooler than the land, as in summer or fall. Cool air near the water surface will tend to increase the stability of the boundary layer in the coastal zone, and thus decrease the mixing processes that act on pollutant emissions. These conditions occur frequently along the New England coast (Hosler, 1961). Similarly, pollutants from the Chicago area have been observed to be influenced by a stable boundary layer over Lake Michigan (Lyons and Olsson, 1972). This has been observed especially in summer and fall when the lake surface is most likely to be cooler than the air that is carried over it from the adjacent land.

Sillman et al. (1993) investigated abnormally high concentrations of O_3 observed in rural locations on the shore of Lake Michigan and on the Atlantic coast in Maine, at a distance of 300 km or more from major anthropogenic sources. A dynamical-photochemical model was developed that represented formation of O_3 in shoreline environments and was used to simulate case studies for Lake Michigan and the northeastern United States. Results suggest that a broad region with elevated O_3, NO_x, and VOC forms as the Chicago plume travels over Lake Michigan, a pattern consistent with observed O_3 at surface monitoring sites. Near-total suppression of dry deposition of O_3 and NO_x over the lake is needed to produce high O_3. Results for the East Coast suggest that the observed peak O_3 can be reproduced only by a model that includes suppressed vertical mixing and deposition over water, 2-day transport of a plume from New York, and superposition of the New York and Boston, MA, plumes. Hence, the thermodynamics associated with the water bodies seem to play a significant role in some regional-scale episodes of high O_3 concentrations.

There is concern that the strict use of mixing height unduly simplifies the complex atmospheric processes that redistribute pollutants within urban areas. There is growing evidence that some O_3 precursors may not be evenly redistributed over some urban areas. These are cases where the sources are relatively close to the urban area and atmospheric mixing is not strong enough to redistribute the material over a short travel time. In these

cases, it is necessary to treat the turbulent structure of the atmosphere directly and acknowledge the vertical variations in mixing. Methods that are being used to investigate these processes include the use of a diffusivity parameter to express the potential for mixing as a function of height. A simple expression of how the mean concentration, $\overline{\chi}$, changes with time, t, in an air parcel, assuming all concentrations are homogeneous in the horizontal, is

$$\frac{d\overline{\chi}}{dt} = -\frac{\partial\overline{w'\chi'}}{\partial z} \quad , \tag{3-80}$$

where $\overline{w'\chi'}$ is the vertical *turbulent eddy flux* of pollutant. The term on the right hand side of the equation changes mean concentration through flux divergence (i.e., turbulence either disperses the pollutant to or from the point being considered). The problem with this representation is that the flux divergence term is virtually impossible to measure directly.

The turbulent eddy flux needed to understand the vertical distribution of O_3 and its precursors often is parameterized in photochemical models, if included at all, through use of *eddy diffusivity*. The eddy diffusivity is set using an analogy to mixing length theory as

$$\overline{w'\chi'} = K_c \frac{\partial\overline{\chi}}{\partial z} \quad , \tag{3-81}$$

which allows estimation of flux divergence from measured or estimated vertical gradients in concentration and estimation of the eddy diffusivity. The selection of diffusivity is often somewhat arbitrary, but can be related to the eddy diffusivity for heat or momentum, depending on circumstances. Large values result in rapid mixing. Thus, the appropriate selection of eddy diffusivity is necessary to simulate whether elevated plumes will enter an urban airshed.

The use of an eddy diffusivity approach to turbulent diffusion assumes local down-gradient diffusion, a situation not always realistic in the atmosphere. It is important to note that eddy diffusivity is not valid under convective conditions because counter-gradient flows occur (Sun, 1986). Eddy diffusivity also does not work in the presence of multiple stable layers. Moreover, the form of the eddy diffusivity used in the existing air quality models is rather arbitrary. More research will be needed to remove this arbitrariness.

Another method used for convective situations is a technique called "large-eddy simulation", employed to recreate the probability of redistribution within the mixing height. This method explicitly simulates the larger eddies occurring under convective situations. These techniques require meteorological information that is not normally available from the National Weather Service but that is now becoming available as part of several O_3 field experiments.

3.3.1.3 Cloud Venting

Vertical redistribution of O_3 out of the PBL is achieved by the venting of pollutants in clouds. Clouds represent the top-most reaches of thermals of air rising through the PBL and can act as chemical reactors for soluble pollutants, returning the "processed" air to the PBL. They also can result in physical redistribution of O_3 and its precursors from the

PBL if convection is sufficiently vigorous (Greenhut, 1986; Dickerson et al., 1987). Clouds also act to influence photolysis rates and chemical transformation rates.

Greenhut (1986) showed that the net O_3 flux in the cloud layer was a linear function of the difference in O_3 concentration between the boundary and cloud layers. Ozone fluxes between clouds were usually smaller than those found within clouds, but the slower rate is at least partially offset by the larger region of cloud-free air relative to cloudy air.

Large clouds, such as cumulonimbus, offer considerably more potential for redistribution of O_3 and its precursors. Additionally, the cumulonimbus clouds also are associated with precipitation, a scavenger of pollutants, and with lightning, a potential source for NO_x. Using CO as a tracer, Dickerson et al. (1987) and Pickering et al. (1990) have illustrated the redistribution potential of cumulonimbus cloud systems. Lyons et al. (1986) provided an illustration of the potential for groups of cumulonimbus clouds to vent the polluted boundary layer.

The role of cloud venting is thought to be largely a cleansing process for the boundary layer, although a portion of the material lifted into the free troposphere could be entrained back to the surface in subsequent convection. Aircraft observations frequently have documented the occurrence of relatively high O_3 concentrations above lower concentration surface layers (e.g., Westberg et al., 1976). This is a clear indication that O_3 is preserved essentially in layers above the surface and can be transported over relatively long distances, even when continual replenishment through precursor reactions is not a factor, such as at night.

3.3.1.4 Stratospheric-Tropospheric Ozone Exchange

The fact that O_3 is formed in the stratosphere, mixed downward, and incorporated into the troposphere, where it forms a more or less uniformly mixed background concentration, has been known in various degrees of detail for many years (Junge, 1963). The mechanisms by which stratospheric air is mixed into the troposphere have been examined by a number of authors, as documented previously by the U.S. Environmental Protection Agency (EPA) (U.S. Environmental Protection Agency, 1986a, and references therein).

Although the portion of background O_3 near the surface attributed to stratospheric-tropospheric O_3 can be in the 5 to 15 ppb range for a seasonal average, this amount of O_3 by itself cannot account for peak urban O_3 values or regional episodes of elevated O_3 levels (Johnson and Viezee, 1981; Ludwig et al., 1977; Singh et al., 1980; and Viezee et al., 1979). Johnson and Viezee (1981) concluded that the O_3-rich intrusions studied sloped downward toward the south. In terms of dimensions, the average crosswind width (north to south), at an altitude of 5.5 km (ca. 18,000 ft), for six spring intrusions, averaged 226 km, and, for four fall tropopause fold systems, averaged 129 km. Ozone concentrations at 5.5 km averaged 108 ppb in the spring systems and 83 ppb in the fall systems. From this and other research described in the previous criteria document for O_3 and other photochemical oxidants (U.S. Environmental Protection Agency, 1986a), Viezee and coworkers (Viezee and Singh, 1982; Viezee et al., 1983) concluded (1) that direct ground-level impacts by stratospheric O_3 may be infrequent, occurring <1% of the time; (2) that such ground-level events are short-lived and episodic; and (3) that they are most likely to be associated on a 1- to 4-h average with O_3 concentrations in the range 60 to 100 ppb.

The monthly stratospheric-tropospheric total O_3 flux from tropospheric folding events in the Northern Hemisphere has been estimated. These fluxes, in units of 10^{35} O_3 molecules per month per tropospheric folding event, increase from 1.0 in January to

2.1 in April and May, decline to 1.0 in August, and reach a minimum of 0.5 in October and November (Viezee et al., 1983). The spring-to-fall variation resembles the seasonal variations of O_3 near ground-level often observed at more remote sites (e.g., Logan, 1985). Four of the 10 episodes in which ground-level O_3 has been attributed to stratospheric O_3 transport occurred during March, but several such episodes during summer months have been reported (see below).

Using the ^{7}Be-to-O_3 ratio as an indicator of O_3 of stratospheric origin and SO_4^{2-} concentrations as a tracer for anthropogenic sources, Altshuller (1987) estimated stratospheric contributions of O_3 in the range 0 to 40 ppb (0 to 95% of observed O_3) at ground level at Whiteface Mountain, NY, for July 1975 and mid-June to mid-July 1977. Monthly average stratospheric contributions were estimated at 5 to 10 ppb. Extant ^{7}Be and O_3 data for a number of lower-elevation rural locations in the western, midwestern, and southeastern United States also were examined, and stratospheric or upper tropospheric contributions of 6 to 8 ppb were calculated. The author concluded that the calculated values for such contributions should be viewed with caution and regarded as probable upper limits because of scatter in the ^{7}Be and corresponding O_3 data that hindered definition of the ^{7}Be-to-O_3 ratio. Altshuller also concluded that removal and dilution processes result in the loss of most stratospheric O_3 before it reaches ground level. In other work performed in England, O_3 of stratospheric origin was estimated to contribute 10 to 15 ppb to the daily maximum hourly mean O_3 concentrations in an April through October period (Derwent and Key, 1988; United Kingdom Photochemical Oxidant Review Group, 1993).

3.3.2 Meteorological Parameters

This section focuses on analyses of data from previous and ongoing measurement programs to address two key questions: (1) are there meteorological parameters which are systematically associated with O_3 levels? and (2) are relationships between O_3 and meteorological parameters sufficiently strong such that meteorological fluctuations can be filtered from the data to allow examination of longer term trends?

The meteorological factors that theoretically could influence surface O_3 levels include ultraviolet radiation, temperature, wind speed, atmospheric mixing and transport, and surface scavenging. The following examines the theoretical basis for each of these factors and identifies to what degree empirical evidence supports the hypotheses.

3.3.2.1 Sunlight

Ultraviolet radiation plays a key role in initiating the photochemical processes leading to O_3 formation. Sunlight intensity (specifically the UV portion of sunlight) varies with season and latitude, but the latter effect is strong only during winter months. The importance of photolysis to the formation of O_3 provides a direct link between O_3 and time of year. However, during the summer, the maximum UV intensity is fairly constant throughout the contiguous United States, and only the duration of the solar day varies to a small degree with latitude.

The effects of light intensity on individual photolytic reaction steps and on the overall process of oxidant formation have been studied in the laboratory (Peterson, 1976; Demerjian et al., 1980). Early studies, however, employed constant light intensities, in contrast to the diurnally varying intensities that occur in the ambient atmosphere. The diurnal variation of light intensity was subsequently studied as a factor in photochemical oxidant

formation (e.g., Jeffries et al., 1975, 1976). Such studies showed that the effect of this factor varies with initial reactant concentrations. Most important was the observation that similar NMOC/NO_x systems showed different oxidant-forming potential depending on whether studies of these systems were conducted using constant or diurnal light. This led to incorporation of the effects of diurnal or variable light into photochemical models (Tilden and Seinfeld, 1982).

There is little empirical evidence in the literature, however, linking day-to-day variations in observed UV radiation levels with variations in O_3 levels. Samson and Shi (1988) illustrated that the number of O_3 concentrations exceeding 120 ppb did not track well with potential solar radiation, as shown in Figure 3-8. Although variations in day-to-day concentrations could well be influenced by cloud cover or attenuated by haze, the seasonal peak in O_3 concentrations usually lags the peak in potential solar radiation that occurs at the Summer Solstice on or about June 23.

3.3.2.2 Temperature

There is an association between tropospheric O_3 concentration and tropospheric temperature that has been demonstrated from measurements in outdoor smog chambers and from measurements in ambient air. A linear relationship between maximum O_3 and temperature was obtained in the smog chambers with little scatter around the regression line (Kelly and Gunst, 1990). Numerous ambient studies done over more than a decade have reported that successive occurrences or episodes of high temperatures characterize seasonally high O_3 years (Clark and Karl, 1982; Kelly et al., 1986). The relationship has been observed for the South Coast Air Basin of California (Kuntasal and Chang, 1987), in New England (Wolff and Lioy, 1978; Atwater, 1984; Wackter and Bayly, 1988), and elsewhere.

Figures 3-9 and 3-10 show the daily maximum O_3 concentrations versus maximum daily temperature for summer months (May to October), 1988 to 1990, for Atlanta and New York City, NY, and for Detroit, MI, and Phoenix, AZ, respectively. There appears to be an upper-bound on O_3 concentrations that increases with temperature. Likewise, Figure 3-11 shows that a similar qualitative relationship exists between O_3 and temperature even at a number of rural locations.

The notable trend in these plots is the apparent upper-bound to O_3 concentrations as a function of temperature. It is clear that, at a given temperature, there is a wide range of possible O_3 concentrations because other factors (e.g., cloudiness, precipitation, wind speed) can reduce the O_3 production. The upper bound presumably represents the maximum O_3 concentration achieved under the most favorable conditions. These plots, based on ambient air measurements, show wide scatter in O_3 concentration with temperature because of the contributions to variations from several of these factors that do not influence the results from smog chamber studies (Kelly and Gunst, 1990). Table 3-4 lists the results of a statistical regression performed on the paired O_3-temperature data used in Figures 3-9 and 3-10 with separate slopes listed for temperatures above and below 30 °C. Results show that, for T > 30 °C, the O_3-temperature relationship is statistically significant at all sites. The rate of increase for T > 30 °C is 3 to 5 ppb/°C at eastern United States rural sites and ranges from 4 to 9 ppb/°C at the three eastern U.S. urban sites (New York, Detroit, and Atlanta). At two western sites, Williston, ND, and Billings, MT, there is a much weaker

Figure 3-8. The number of reports of ozone concentrations ≥120 ppb at the 17 cities studied in Samson and Shi (1988). (1 April = Week 14, 1 May = Week 18, 1 June = Week 22, 1 July = Week 27, 1 August = Week 31, 1 September =

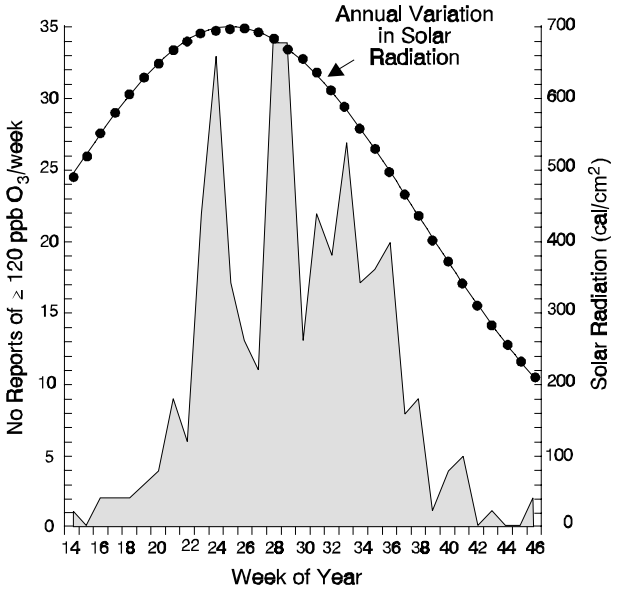

Week 35, 1 October = Week 40, 1 November = Week 44). A representation of the annual variation in solar radiation reaching the earth's surface at 40°N latitude (units = cal cm^{-2}) is shown.

Source: Samson and Shi (1988).

dependence on temperature, possibly reflecting the lower level of anthropogenic activity. At a third western site, Medford, OR, the O_3-temperature relationship is comparable to that at rural eastern sites.

Relationships between peak O_3 and temperature also have been recorded by Wunderli and Gehrig (1991) for three locations in Switzerland. At two sites near Zurich, peak O_3 increased 3 to 5 ppb/°C for diurnal average temperatures between 10 and 25 °C, and little change in peak O_3 occurred for temperatures below 10 °C. At the third site, a high-altitude location removed from anthropogenic influence, much less variation of O_3 with temperature was observed.

The hypotheses for this correlation of O_3 with temperature include, but are not necessarily limited to:

1. Reduction in photolysis rates under meterological conditions associated with low temperatures;
2. Reduction in H_2O concentrations at low temperatures;
3. Thermal decomposition of PAN and its homologues;
4. Increased anthropogenic emissions of reactive hydrocarbons or NO_x, or both;
5. Increased natural emissions of reactive hydrocarbons; and
6. Relationships between high temperatures and stagnant circulation patterns.

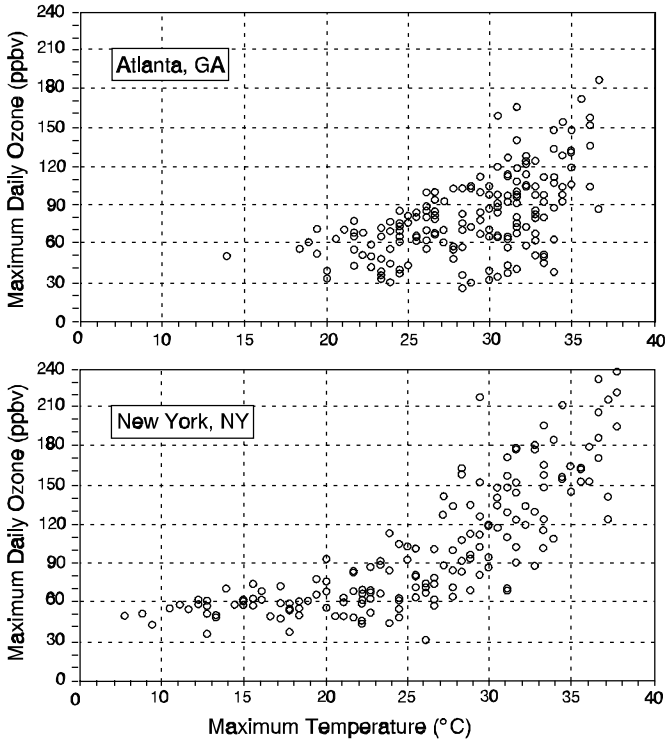

Figure 3-9. A scatter plot of maximum daily ozone concentration in Atlanta, GA, and New York, NY, versus maximum daily temperature.

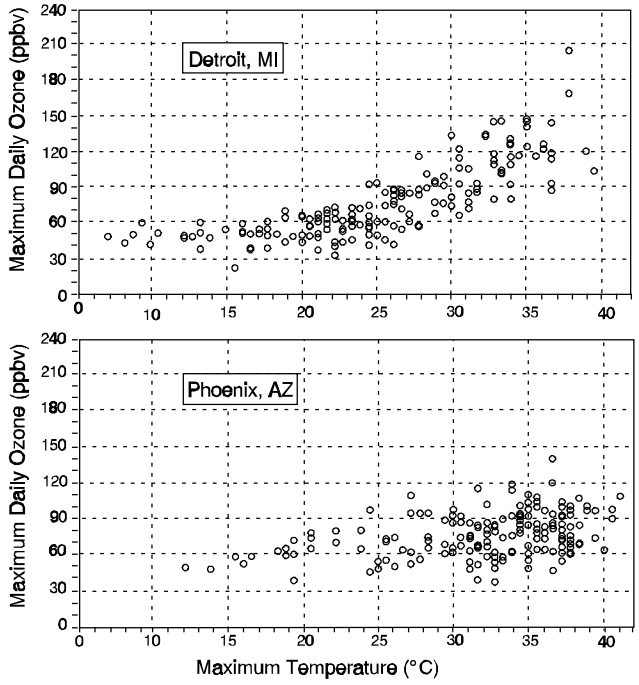

Figure 3-10. A scatter plot of maximum daily ozone concentration in Detroit, MI, and Phoenix, AZ, versus maximum daily temperature.

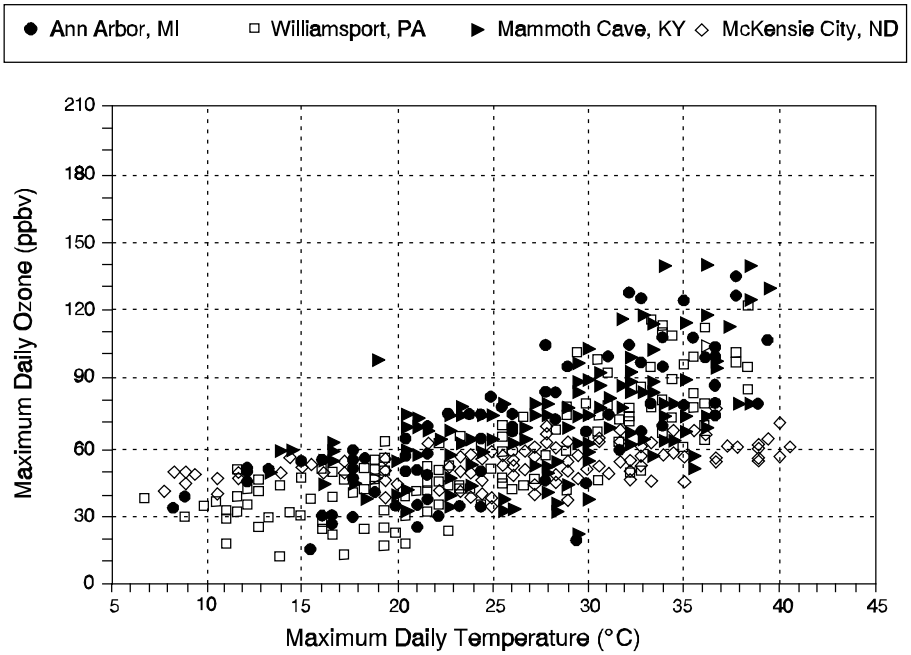

Figure 3-11. A scatter plot of maximum ozone concentration versus maximum daily temperature for four nonurban sites. The relationship with temperature is still apparent, although the slope is reduced from that of the urban areas.

Table 3-4. Rates of Increase of Peak Ozone with Diurnal Maximum Temperature (ppb/°C) for Temperature <300 K (27 °C) and Temperature >300 K, Based on Measurements for April 1 to September 30, 1988[a]

Location		T < 300 K		T > 300 K	
		$\Delta O_3/\Delta T$	T-Statistic	$\Delta O_3/\Delta T$	T-Statistic
Urbanized Regions					
	NY-NJ-CT	1.5	−5.2	8.8	−7.4
	Detroit	1.4	−6.4	4.4	−6.3
	Atlanta	3.2	−4.2	7.1	−5.9
	Phoenix	—	—	1.4	−4.1
	Southern California	11.3	−8.9	—	—
Nonurban Sites					
	Williamsport, PA	1.2	−5.0	4.0	−7.4
	Saline, MI	0.8	−3.5	3.1	−4.9
	Mammoth Cave, KY	0.1	−0.3	4.4	−7.3
	Kentucky, cleanest site 3	0.3	−0.7	3.4	−6.6
	Williston, ND	0.2	−1.0	0.8	−3.7
	Billings, MT	0.1	−0.5	0.7	−2.2
	Medford, OR	0.5	−2.6	3.3	−13.7

[a]See Appendix A for abbreviations and acronyms.

The relationship with temperature is well known, but not yet reproduced by air quality models. Although it has been argued that this striking relationship with temperature is an indirect result of the stagnant synoptic meteorological conditions that lead to higher O_3 levels, the correlation is not strong with other parameters of stagnation, notably wind speed, which is discussed later.

Reduction in Photolysis Rates

It is possible that, on a seasonal scale, the correlation between temperature and O_3 may be an indirect correlation with UV radiation variability. This is insufficient, however, to explain the day-to-day correlation between the two variables.

Changes in photolysis rates and in H_2O concentrations are related in that both are linked to the supply of OH radicals, which determines the rate of O_3 production in clean atmospheres and contributes to O_3 production in polluted atmospheres. A reduction in either photolysis rates or H_2O would reduce the source of OH radicals. Calculations by Sillman and Samson (1995) showed that the difference between summer and fall photolysis rates (at 40° N latitude) has a significant impact on the rate of O_3 production in urban photochemical simulations, roughly equal to the impact of PAN thermal decomposition (discussed below). However the impact of photolysis rates and of water vapor was much lower in simulations for polluted rural environments. In the simulations by Sillman et al. (1993), O_3 production in urban environments was limited largely by the supply of OH radicals to react with hydrocarbons; whereas in rural environments the limiting factor was the source of NO_x. Consequently, photolysis rates and H_2O had less impact on O_3 production in rural environments.

Thermal Decomposition of Peroxyacetyl Nitrate

Temperature-dependent photochemical rate constants provide a link between O_3 and temperature (Sillman et al., 1990a; Cardelino and Chameides, 1990). The reason for the decline in O_3 in rural areas when the PAN decomposition rate decreases is that PAN represents a sink for NO_x in rural environments. When the rate of PAN decomposition is decreased, NO_x drops sharply, whereas OH and HO_2 remain largely unaffected. Consequently, the rate of the important HO_2 + NO reaction (see Section 3.2) shows a substantial decrease.

The photochemical response in an urban environment is fundamentally different, although the final result, a decrease in O_3 with temperature, is similar. The impact of PAN in urban environments is attributable to its role as a sink for odd hydrogen rather than to its effect on NO_x (Cardelino and Chameides, 1990). Sillman et al. (1990a) have shown that the well-known division of O_3 photochemistry into NO_x- and VOC-sensitive regimes is associated with the relative magnitude of odd-hydrogen sinks.

Sillman and Samson (1995) found that the thermal decomposition of PAN was enough to explain an increase of 1 to 2 ppb peak O_3/°C increase in temperature in rural locations in the eastern United States, based on photochemical simulations. This increase represents a significant fraction of the observed increase in peak O_3 with a rise in temperature (3 to 5 ppb/°C, Table 3-4).

Increased Anthropogenic Emissions

Emission rates for anthropogenic hydrocarbons (VOCs) also can increase with temperature (U.S Environmental Protection Agency, 1989; Stump et al., 1992). Increased

anthropogenic VOC emissions might be expected to cause increased rates of O_3 production in urban areas where O_3 is sensitive to VOC, but would be less likely to have impact on rural areas where biogenic VOC emissions can predominate. However, O_3 in rural areas is NO_x dependent. The NO_x-sensitive rural areas also would show increased O_3 production with a rise in temperature as biogenic NO_x emissions increase with temperature.

Increased Natural Emissions

Emissions of biogenic hydrocarbons increase sharply with a rise in temperature (Lamb et al., 1987). In ambient temperatures from 25 to 35 °C, the rate of natural hydrocarbon emissions from isoprene-emitting deciduous trees increased by about a factor of 4. From coniferous trees, the increase was on the order of 1.5.

Recently, Jacob et al. (1993) found that the photochemistry of O_3 production in a polluted rural environment (Blue Ridge Mountains, VA) is significantly different in September and October, when natural emissions from deciduous forests have ceased. The difference in chemistry between summer and fall leaf production also may have an impact on the O_3-temperature correlation.

Correlation with Stagnation

Recently, Jacob et al. (1993b) found that model-simulated O_3 formation in the rural United States shows a tendency to increase with a rise in temperature, based solely on the difference in atmospheric circulation between relatively warm and relatively cool days. The model-simulated O_3-temperature correlation was less than observed but large enough to represent a significant component of the observed correlation. However, the temperature-meteorology correlation identified by Jacob et al. (1993b) was based on simulated meteorology from a General Circulation Model rather than on direct observations.

3.3.2.3 Wind Speed

Ozone is expected to be influenced by wind speed because lower wind speeds should lead to reduced ventilation and the potential for greater buildup of O_3 and its precursors. Abnormally high temperatures are frequently associated with high barometric pressure, stagnant circulation, and suppressed vertical mixing resulting from subsidence (Mukammal et al., 1982), all of which may contribute to elevated O_3 levels. However, in reality this relationship varies from one part of the country to another. Figure 3-12 shows the frequency of 24-h trajectory transport distances to Southern cities on days with resulting concentrations of $O_3 \geq 120$ ppb (Samson and Shi, 1988). The frequency for Southern cities is biased toward lower wind speeds. The same bias was shown for all 17 cities in the study. A similar plot for cities in the northeastern United States (Figure 3-13) shows an opposite pattern, in which the bias is toward higher wind speeds than normal. It is unclear how much meteorological information is needed in order to perform accurate urban-area O_3 simulations using advanced photochemical models. To understand the significance of variations between upper-air wind measurements during the Southern Oxidant Study (SOS), 1992, Atlanta, an intensive, intercomparison test of the precision of upper-air measurements was conducted. Collocated measurements were made at an SOS measurement site, using a boundary-layer lidar, a wind profiler, and a rawinsonde balloon. There was generally good agreement between the profiler and rawinsonde, although some large outliers existed. Figure 3-14 illustrates that the root-mean-square difference (RMSD) varied with altitude. The RMSD reached a minimum near 1,200 m above ground level (AGL) of about 2 m/s, rising to over

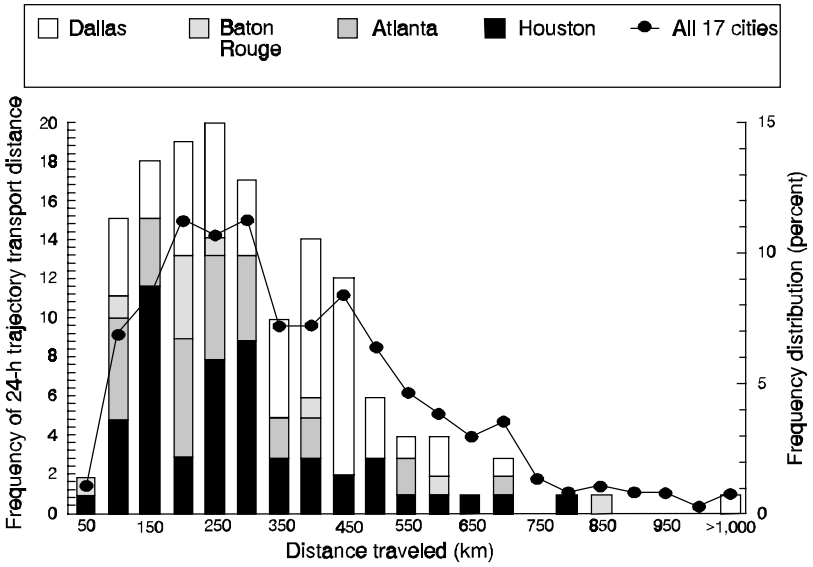

Figure 3-12. The frequency of 24-h trajectory transport distance en route to city when ozone was ≥120 ppb in four Southern U.S. cities, compared with the percent frequency distribution for all 17 cities (scale on right) of a nationwide study, 1983 to 1985.

Source: Samson and Shi (1988).

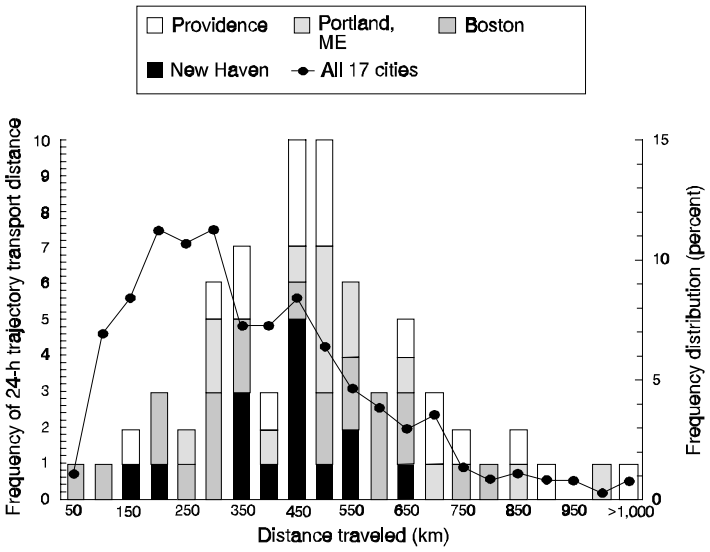

Figure 3-13. The frequency of 24-h trajectory transport distance en route to city when ozone was ≥120 ppb in four New England cities, compared with the percent frequency distribution for all 17 cities (scale on right) of a nationwide study, 1983 to 1985.

Source: Samson and Shi (1988).

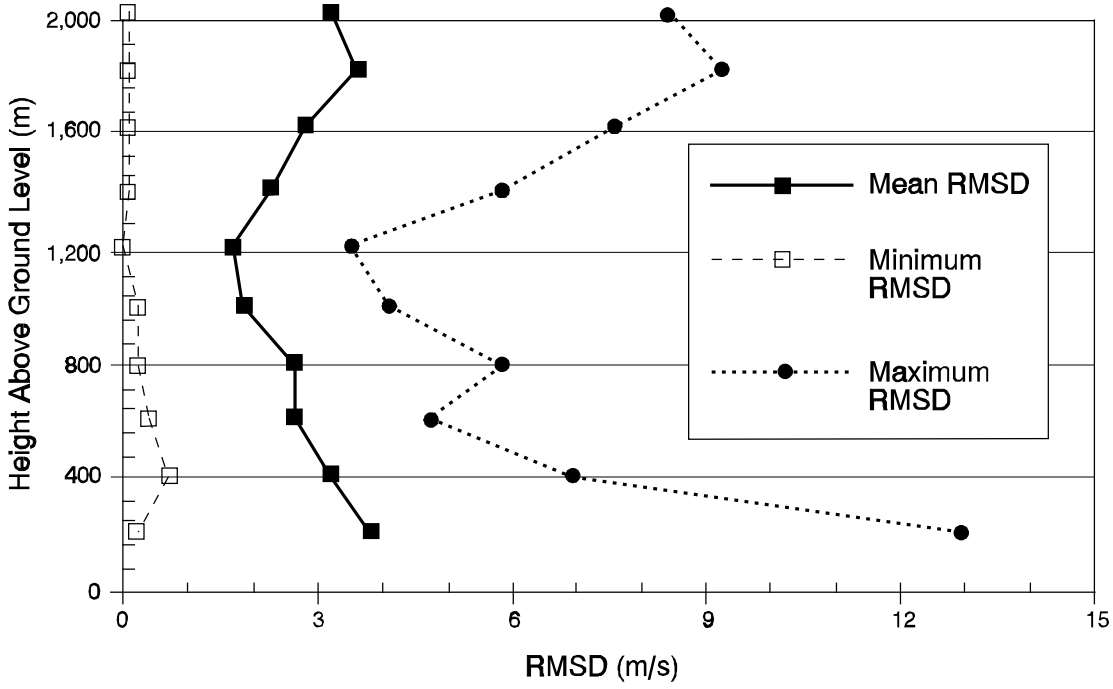

Figure 3-14. The root-mean-square difference (RMSD) between CLASS observations and profiler observations as a function of height above ground level.

3 m/s near the surface and above 1,200 m AGL. Figure 3-15 illustrates the RMSD for the lidar comparison with CLASS observations. There is slightly greater RMSD at all heights than for the profiler-rawinsonde comparison, with a relative minimum observed at about 1,200 m.

Although the measurements were significantly correlated, the results illustrate that there was still considerable disagreement between methods. The profiler had better precision than the lidar had, although the differences were negligible if the first four runs were excluded from the data set. The profiler obtained values biased slightly higher than the CLASS system (+0.2 m/s), whereas the lidar system was biased low (−0.3 m/s or −0.5 m/s). The statistical comparisons of both the profiler and the boundary-layer lidar with the rawinsonde system suggest that variations in wind speed at a particular level must be larger than about 3 m/s to be considered significant.

3.3.2.4 Air Mass Characteristics

In meteorology, an "air mass" is a region of air, usually of multistate dimensions, that exhibits similar temperature, humidity, or stability characteristics. Air masses are created when air becomes stagnant over a "source region" and subsequently takes on the characteristics of the source region. Similarly, when dealing with air pollution meteorology, it is possible to identify a "chemical air mass" as a region of air that has become stagnant over an emissions source area. Air that is stagnant over, say, the center of Canada will exhibit relatively cold, dry conditions and will be relatively devoid of pollutants. Air that

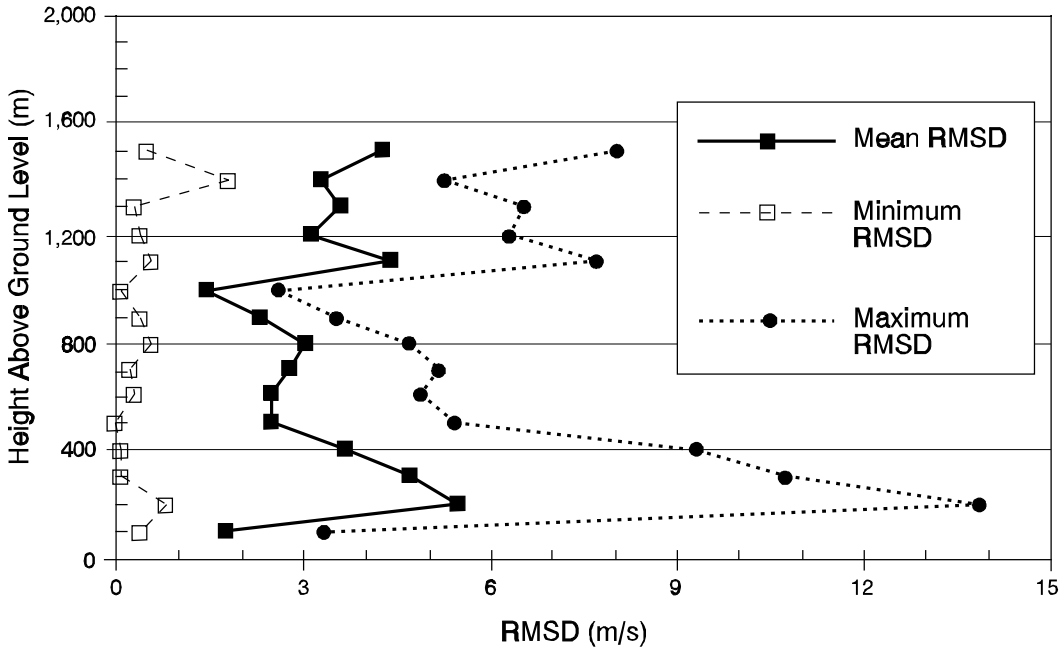

Figure 3-15. The root-mean-square difference (RMSD) between CLASS observations and lidar observations as a function of height above ground level.

resides over the industrial regions of the midwestern United States will exhibit low visibility and, often, high O_3 levels on a regional scale. Meteorological processes play an important role in determining the amount of "accumulation" of O_3 and its precursors that occurs under such stagnant conditions.

Episodes of high O_3 concentrations in urban areas often are associated with high concentrations of O_3 in the surroundings. This accumulated O_3 forms under the same atmospheric conditions that lead to high O_3 levels in urban areas and exacerbates the urban problem by supplying relatively high O_3 and precursor concentrations to the urban area from upwind. The transport of O_3 and its precursors beyond the urban scale ($\leq$50 km) to neighboring rural and urban areas has been well documented (e.g., Wolff et al., 1977a,c; Wolff and Lioy, 1978; Clark and Clarke, 1984; Sexton, 1982; Wolff et al., 1982; Altshuller, 1988). A summary of most of these reports was given in the 1986 O_3 criteria document (U.S. Environmental Protection Agency, 1986a) and will not be reiterated here. The phenomena of high nonurban O_3 levels was illustrated by Stasiuk and Coffey (1974) for transport within New York State; by Ripperton et al. (1977) for sites in the Middle Atlantic States; and by Samson and Ragland (1977) for the midwestern United States.

These areas of O_3 accumulation are characterized by synoptic-scale subsidence of air in the free troposphere, resulting in development of an elevated inversion layer; relatively low wind speeds associated with the weak horizontal pressure gradient around a surface high pressure system; lack of cloudiness; and high temperatures.

On occasion, O_3 at levels greater than 120 ppb can occur in rural areas far removed from urban or industrial sources. Ozone levels at the summit of Whiteface Mountain exceeded this value during the summer of 1988 when O_3 accumulated across a

wide expanse of the eastern United States at levels ≥120 ppb. Nonetheless, even when the regional accumulation is at a level below the current O_3 NAAQS, the increment needed to bring the level above the NAAQS in an urban area is not large.

The identification and understanding of the transport of photochemical O_3 and other oxidants and their precursors by weather systems represent a significant advance in comprehending photochemical air pollution and the potential extent of its effects. Considerable progress has been made in the development of long-range photochemical modeling techniques so that the likely impact of synoptic systems can be anticipated. Such tools are very much in the research stage, however, because the local impact of O_3 and other oxidants results from a complex interaction of distant and local precursor sources, urban plumes, mixing processes, atmospheric chemical reactions, and general meteorology.

3.3.3 Normalization of Trends

The degree to which meteorological factors can be "normalized" out of the O_3 concentration and "trends" data depends in large part on the strength of the relationships between O_3 and meteorological components. As part of the SOS Atlanta intensive field campaign, an attempt was made to model statistically the O_3 levels in Atlanta to build a predictive tool for forecasting days of specialized measurement. Figure 3-16 shows the fit of the data used to create the model to the model simulations. Figure 3-17 shows the fit obtained from independent data collected in 1992.

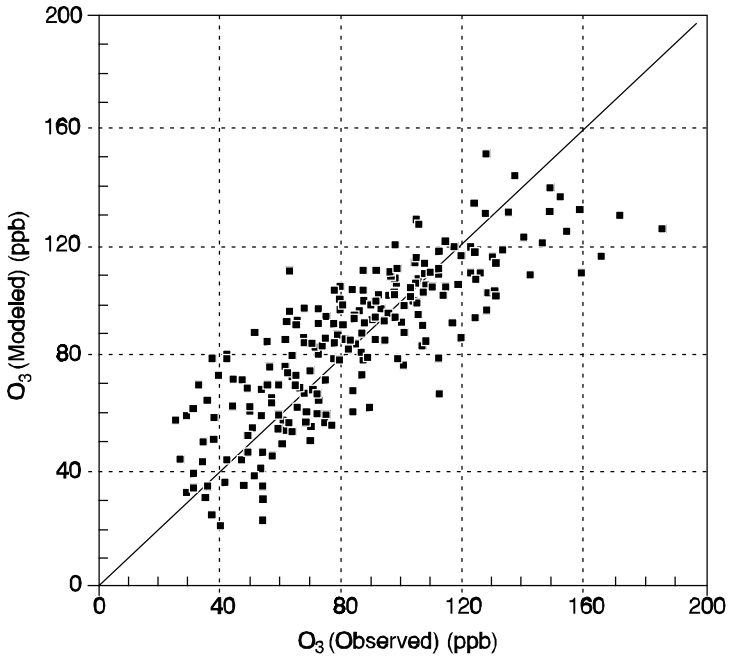

Figure 3-16. Model of ozone (O_3) levels using regression techniques. The use of wind speed, temperature, and previous-day ozone provided a means to forecast O_3 levels.

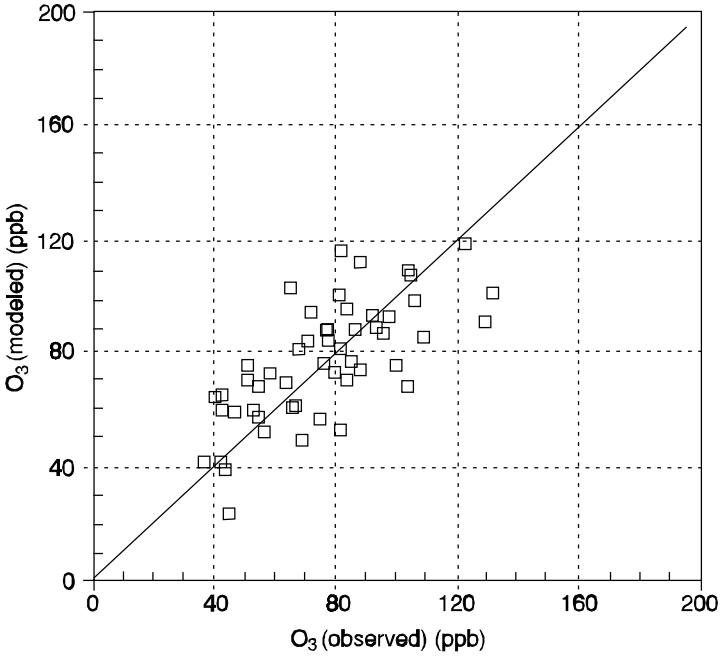

Figure 3-17. Simulated versus observed ozone levels using regression techniques on an independent data set obtained in the summer of 1992 in Atlanta, GA.

This model was used successfully to predict next-day O_3 levels in Atlanta. Ozone levels in a number of American cities should be analyzed using regression tools such as this in order to normalize meteorological variability. Through such analyses, it is possible that trends, if any, represented as systematic deviations from the model, may become observable. A summary of other techniques for removing meteorological variability is contained in the recent monograph from the National Research Council (1991). Table 3-5 lists a sample of studies aimed at evaluation of O_3 trends.

3.4 Precursors of Ozone and Other Oxidants

3.4.1 Sources and Emissions of Precursors

3.4.1.1 Introduction

As described elsewhere in this chapter, O_3 is formed in the atmosphere through a series of chemical reactions that involve VOCs and NO_x. Control of O_3 depends on reducing emissions of VOCs or NO_x or both. Thus, it is important to understand the sources and source strengths of these precursor species in order to devise the most appropriate oxidant control strategies. In the following sections, anthropogenic and biogenic NO_x and VOC sources will be described, and the best estimates of their current emission levels and trends will be provided. Confidence levels for the assigned source strengths will be discussed.

Both English and metric units have been utilized in emission inventories. Thousands or millions of short tons are the common scales in the English system. The metric unit most

Table 3-5. Recent Studies Examining Trends in Ozone Data After Removal of Variability Associated with Meteorological Factors

Study	Variables	Approach
Jones et al. (1989)	Surface temperature	Compared number of days with ozone concentrations above 120 ppb to days with temperature above 30 °C.
Pollock et al. (1988)	Surface temperature	Compared number of days with ozone concentrations above 105 ppb to days with temperature above 30 °C.
Kuntasal and Chang (1987)	850-mb temperature	Regression of ozone versus temperature for Southern California.
Wakim (1989)	Surface temperature	Regression of ozone versus temperature for Houston, New York, and Washington, DC.
Chock et al. (1982)	Surface temperature, wind speed, relative humidity, sky cover, wind direction, dew point temperature, sea level pressure, precipitation.	Regression versus a variety of meteorological parameters.
Kumar and Chock (1984)	Surface temperature, wind speed, relative humidity, sky cover, wind direction, dew point temperature, sea level pressure, precipitation.	Regression versus a variety of meteorological parameters.
Korsog and Wolff (1991)	Surface temperature, wind speed, relative humidity, sky cover, wind direction, dew point temperature, sea level pressure, precipitation.	Regression versus a variety of meteorological parameters.

Source: National Research Council (1991).

often employed is millions of metric tons, which is equivalent to teragrams (Tg). To convert English tons to teragrams, multiply English tons by 0.907×10^{-6}. For consistency, teragrams have been employed throughout the ensuing discussion.

3.4.1.2 Nitrogen Oxides

Manmade Emission Sources

Anthropogenic NO_x sources are associated with combustion processes. The primary pollutant is NO, which is formed from nitrogen and oxygen atoms that are produced at high combustion temperatures when air is present. In addition, NO_x is formed from nitrogen contained in the combustion fuel. Major NO_x source categories include transportation, stationary source fuel combustion, industrial processes, solid waste disposal,

and some miscellaneous combustion-related activities. Table 3-6 provides a more detailed summary of each of these source categories. The transportation category includes gasoline- and diesel-powered motor vehicles, aircraft, railcars, vessels, and off-highway vehicles. Electric utilities, industrial and commercial/institutional boilers, industrial furnaces, and space heaters comprise the stationary source fuel combustion category. Industrial processes include petroleum refining and paper, glass, steel, cement, and chemical production. The incineration and open burning of waste leads to emissions of NO_x in the solid waste disposal category. The miscellaneous sources category includes prescribed forest slash burning, agricultural burning, coal refuse burning, and structure fires. It should be noted at this point that, even though NO is the pollutant emitted, NO_x emission inventories are quantified relative to NO_2 (mol wt = 46). Nitrogen dioxide is a secondary pollutant produced via oxidation of NO in the atmosphere.

Quantifying NO_x emissions in all of these categories generally requires multiplying an emission factor and an activity level. Nitrogen oxides emission factors are obtained from *Compilation of Air Pollution Factors*, AP-42 (U.S. Environmental Protection Agency, 1985), and from the current mobile source emission factor model (e.g., MOBILE5) recommended by EPA. Activity levels are derived from information sources that provide consumption levels. This takes the form of fuel type and amount consumed for stationary sources and, for transportation sources, the number of vehicle miles traveled (VMT). Point-source emissions are tallied at the individual plant level. These plant-by-plant NO_x emissions are first summed at the state level, and then state totals are added to arrive at the national emissions total. Data on VMT are published for three road categories: (1) highways, (2) rural roads, and (3) urban streets.

Table 3-7 provides a summary of NO_x emissions from the various categories mentioned previously (U.S. Environmental Protection Agency, 1993b). The 1991 total is 21.39 Tg of NO_x emissions in the United States. About half of the emissions (10.69 Tg) is associated with the stationary source fuel combustion category. Transportation-related activities are the second largest source, accounting for about 45% of the national total. The remaining 7% of emissions are divided among the industrial processes, solid waste disposal, and miscellaneous sources categories. The two largest single NO_x emission sources are electric power generation and highway vehicles. Local NO_x source apportionment may differ substantially from these national figures.

Because of the dominance of the electric utility and transportation sources, the geographical distribution of NO_x emissions is related to areas with a high density of power-generating stations and urban regions with high traffic densities. Figure 3-18 shows the location of the 50 largest electric power generating sources of NO_x in the United States. The majority of these power plants are concentrated in the upper Mississippi-Ohio River corridor. Because of this congregation of large point sources, 69% of U.S. NO_x emissions occur within U.S. Environmental Protection Agency Regions III, IV, V, and VI (Figure 3-19). It is interesting to compare the annual NO_x emissions from a large electrical generating plant with the yearly transportation-related emissions in a major metropolitan region. The largest utility plants currently release between 0.06 and 0.09 Tg of NO_x annually, which compares to approximately 0.12 Tg of NO_x emitted by transportation sources in the Atlanta urban area (U.S. Environmental Protection Agency, 1993b).

Table 3-6. Source Categories Used to Inventory Nitrogen Oxides Emissions

Transportation	Stationary Source Fuel Combustion	Industrial Processes	Solid Waste Disposal	Miscellaneous
Highway vehicles	Coal	Pulp mills	Incineration	Forestries
Gasoline-powered	Electric utilities	Organic chemicals	Open burning	Other burning
Passenger cars	Industrial	Ammonia		
Light trucks - 1	Commercial/Institutional	Nitric acid		
Light trucks - 2	Residential	Petroleum refining		
Heavy-duty vehicles		Glass		
Motorcycles		Cement		
		Lime		
		Iron and steel		
Diesel-powered	Fuel oil			
Passenger cars	Electric utilities			
Light trucks	Industrial			
Heavy-duty vehicles	Commercial/Institutional			
	Residential			
Aircraft	Natural gas			
Railcars	Electric utilities			
Vessels	Industrial			
Farm machinery	Commercial/Institutional			
Construction machinery	Residential			
Industrial machinery				
Other off-highway vehicles				
	Wood			
	Industrial			
	Residential			
	Other Fuels			
	Industrial			
	Residential			

Source: U.S. Environmental Protection Agency (1992a).

Table 3-7. 1991 Emission Estimates for Manmade Sources of Nitrogen Oxides in the United States

Source Category	Emissions (Tg)	
Transportation		9.71
Highway vehicles	7.20	
Off-highway vehicles	2.51	
Stationary fuel combustion		10.69
Electric utilities	6.74	
Industrial	3.27	
Other	0.68	
Industrial processes		0.80
Solid waste disposal		0.07
Miscellaneous		0.12
Forest burning		
Other burning		
Miscellaneous organic solvents		
Total of all sources		21.39

Source: U.S. Environmental Protection Agency (1993b).

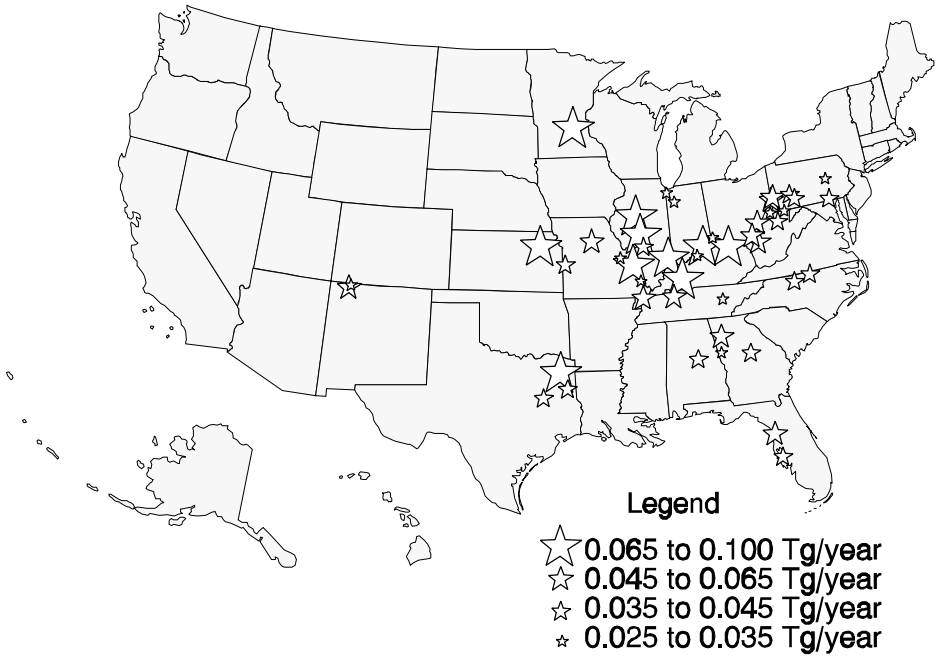

Figure 3-18. The 50 largest sources of nitrogen oxides (power plants) in the United States.

Source: U.S. Environmental Protection Agency (1992a).

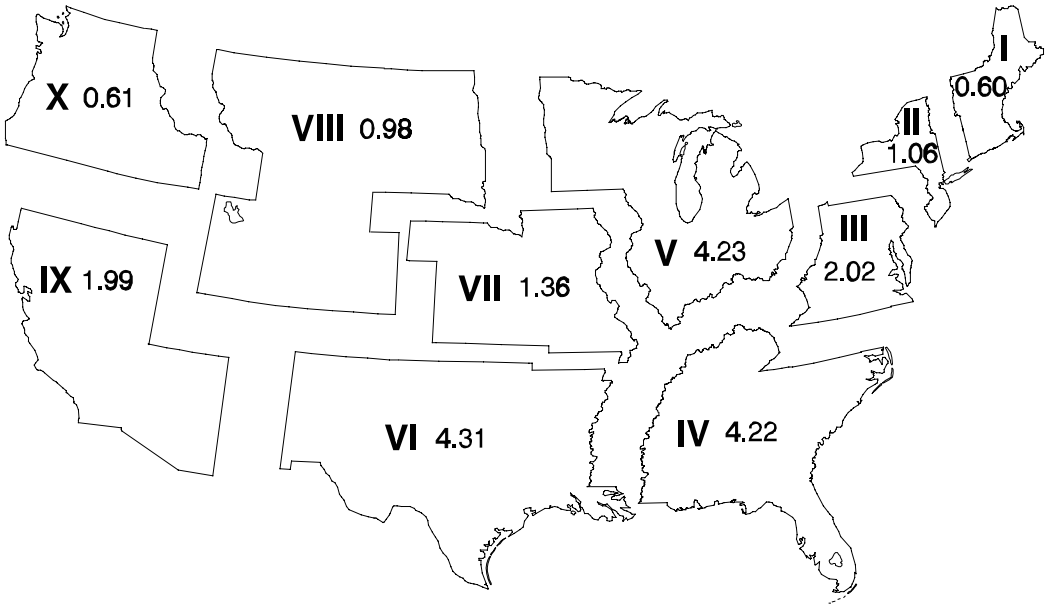

Figure 3-19. Nitrogen oxides emissions (Tg/year) from manmade sources in the 10 U.S. Environmental Protection Agency regions of the United States, 1991.

Source: U.S. Environmental Protection Agency (1993b).

Seasonal variations are available for the 1993 NO_x emissions from 14 source categories in the United States (U.S. Environmental Protection Agency, 1994). Very little seasonal variation occurred for categories contributing approximately three-quarters of the total annual NO_x emissions, including the categories of highway vehicles, electric utilities, and industrial combustion sources. For off-highway sources (comprising 20% of the total annual NO_x emissions), 29% of the off-highway NO_x emissions occur in the summer and 21% in the winter. In contrast, the category of other combustion sources (comprising 5% of the total annual NO_x emissions) emit 47% of the NO_x emissions in the winter and only 8% in the summer. An earlier inventory for 1985 (U.S. Environmental Protection Agency, 1989), which considered only total point and area anthropogenic NO_x emissions, indicated that very little variation occurred in NO_x emissions among the winter, spring, summer, and fall seasons. The contributions of these NO_x categories also were shown to vary seasonally by region of the United States.

Trends in Nitrogen Oxides Emissions

Estimates of NO_x emissions have been made back to 1900, when approximately 2.3 Tg were emitted into the atmosphere in the United States (U.S. Environmental Protection Agency, 1992a). Figure 3-20 summarizes the growth in NO_x emissions at 10-year intervals since the 1940s. Emissions grew rapidly until the 1970s and then leveled off at about

Figure 3-20. Changes in nitrogen oxides emissions from manmade sources in the United States, 10-year intervals, 1940 through 1990.

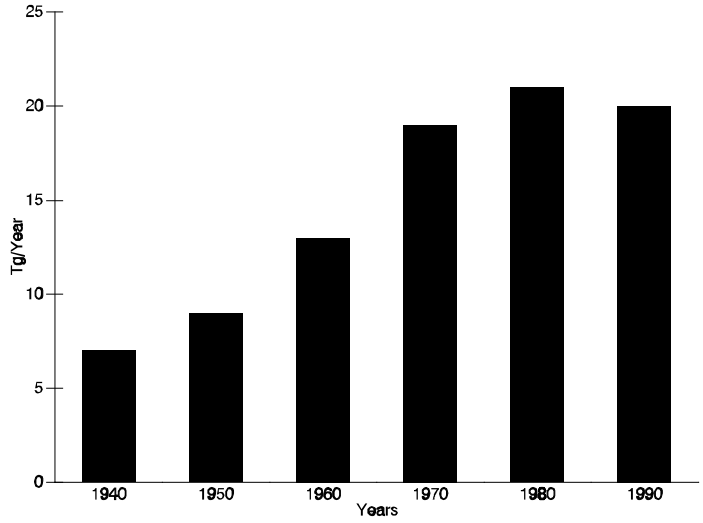

Source: U.S. Environmental Protection Agency (1992a).

20 Tg/year. Currently, more than 90% of the national NO_x emissions result from transportation activities and stationary fuel combustion. Figure 3-21 illustrates the growth in each of these categories over the last 50 years. Transportation-related NO_x emissions grew steadily until the 1980s and then exhibited a moderate decrease. However, the recent trends in transportation-related NO_x emissions shown in Table 3-8 indicate no trend between 1987 and 1991. Emissions of NO_x from fuel combustion sources have increased continually from 1940 to the present time.

Recent trends in the major NO_x emission categories are shown in Table 3-8. Between 1987 and 1991, transportation-related NO_x emissions have remained essentially constant, whereas the stationary source NO_x emissions have increased about 10%.

Transportation and stationary source fuel combustion will likely show downward trends in their NO_x emissions during the next 20 years. This will result from the provisions of the Clean Air Act, which was passed in 1990. Emission limits for electric utility boilers have been prescribed to reduce acidic deposition, automobile tailpipe emission standards will be tightened, and current technology-based applications will be required for industrial boilers (non-utility) in O_3 nonattainment areas. In addition, the average grams of NO_x per mile from passenger cars is expected to decrease because of new on-board diagnostic systems and expanded inspection and maintenance requirements.

As a result of new emission limits and revised performance standards, NO_x emissions from electric utilities are expected to decrease by 16% by the year 2000. Control requirements in the industrial non-utility sector are expected to reduce NO_x emissions by 10% between 1990 and 2000. Projections based on VMT and emission factors from the MOBILE model suggest nearly a 50% decrease in NO_x emissions from highway vehicles manufactured from 1990 to 2000 (U.S. Environmental Protection Agency, 1992a).

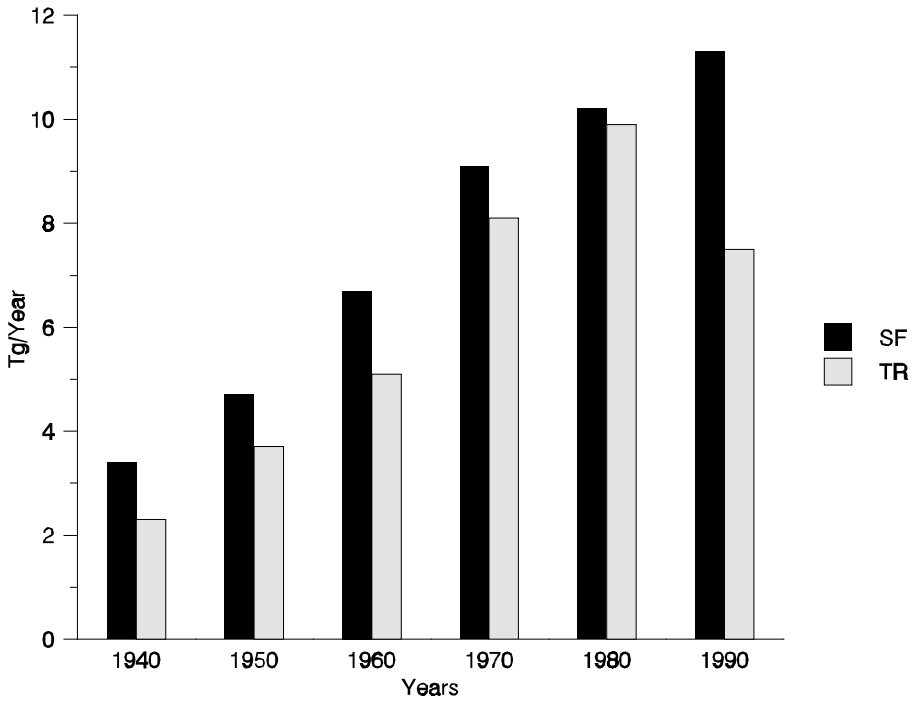

Figure 3-21. Changes in nitrogen oxides emissions from stationary source fuel combustion (SF) and transportation (TR) from 1940 through 1990.[a]

[a]The values for 1990 do not agree with those in Table 3-8 because different models were employed for deriving the short- and long-term trends.

Source: U.S. Environmental Protection Agency (1992a).

Table 3-8. Recent Trends in Nitrogen Oxides Emissions for Major Manmade Source Categories (Tg)

Year	Transportation	Stationary Source Fuel Combustion
1991	9.7	11.0
1990[a]	9.9	10.7
1989	9.7	10.7
1988	9.9	10.6
1987	9.7	10.1

[a]The values for 1990 do not agree with those in Figure 3-21 because different models were employed for deriving the short- and long-term trends.

Source: U.S. Environmental Protection Agency (1993b).

Uncertainty of Anthropogenic Nitrogen Oxides Emission Estimates

Because a large proportion of the U.S NO_x emissions are derived from distinct point sources, it generally is believed that published estimates are very reliable. For example, the National Acid Precipitation Assessment Program (NAPAP) NO_x inventory for U.S. emissions in 1985 (18.6 Tg) was assigned a 90% relative confidence interval in the range of 6 to 11% (Placet et al., 1991). This confidence level was based on judgments used to assign uncertainty to component inputs of emission models and on statistical assumptions used to aggregate uncertainty values.

Sources of error are associated with both the emission factors and the activity levels utilized in the inventorying process. Emission factors provide quantitative estimates of the average rate of emissions from many sources. Consequently, these factors are best applied to a large number of sources over relatively long time periods. In other words, an NO_x emission estimate for a single point source on a particular day in 1990 may be highly inaccurate; but the emission value for this same source for the entire year of 1990 may be very good. It appears that the emission factors assigned to the transportation sectors may be the most uncertain. This results from the emission factors having been derived from mobile source models that require multiple inputs. This type of model requires information on temperatures, vehicle speeds, gasoline volatility, and several other parameters.

Recent attempts to validate NO_x emission factors or inventories have involved comparing ambient NO_x concentrations with values predicted using emissions-based models. These generally have taken one of two forms: (1) comparisons between NO_x concentrations measured in a tunnel and those predicted from emission factors, activity levels, and dilution factors in the tunnel; or (2) whole-city integration procedures in which ambient NO_x concentrations are compared to ambient NO_x levels that have been predicted using a model such as the Urban Airshed Model (UAM). The latter approach has been applied in the South Coast Air Basin (Fujita et al., 1992). It was reported that measured and predicted NO_x concentrations agreed within 20% for a 2-day period in August 1987. Likewise, the results from tunnel studies (Pierson et al., 1990; Robinson et al., 1996) have shown reasonably good agreement between predicted and measured NO_x concentrations. It is important to keep in mind that ambient NO_x levels predicted using a modeling method cannot be assigned true value status. There could be as much or more uncertainty in the model outputs as there is in the emission inputs that are being tested. The fact, however, that an emissions-based model predicts ambient concentrations that are close to those measured tends to lend credence to the NO_x emission estimates. No systematic study of the effect of these uncertainties on model predictions has been published, but a limited summary of sensitivity analyses appears in Seinfeld (1988).

In addition, NO_x inventory validation has involved comparing annual emission estimates reported by different groups. Table 3-9 shows several annual U.S. NO_x emission estimates. In 1982, the estimates vary by less than 12% and this decreases to about 9% in the 1985 comparison.

Natural Emission Sources

Natural sources of NO_x include lightning, soils, wildfires, stratospheric intrusion, and the oceans. Of these, lightning and soils are the major contributors. The convention is to include emissions from all soils in the biogenic or natural category even though cultivated soil emissions are in a sense anthropogenic; cultivated soils also appear to produce higher emissions than those from undisturbed forest and prairie soils, as discussed later. Although

Table 3-9. Comparison of Estimates of Nitrogen Oxides Emissions from Manmade Sources in the United States[a]

	Emissions/year (Tg)	
Inventory	1982	1985
NAPAP	—	18.6
EPA	19.6	19.8
MSCET	18.8	18.2
EPRI	20.7	—

[a]See Appendix A for abbreviations and acronyms.

Source: U.S. Environmental Protection Agency (1993a).

NO_x emitted from large wildfires can be significant on a regional scale, this source is overall considered to be of minor importance for the United States. Injection of NO_x into the upper troposphere via subsidence from the stratosphere is estimated at less than 0.1 Tg/year for all of North America. Because of the relatively short lifetime of NO_x (1 to 3 days) and small NO_x emissions from sea water, transport of NO_x from oceans is thought to be a negligible source in the United States.

Lightning. Lightning produces high enough temperatures to allow N_2 and O_2 to be converted to NO. Two methods have been employed to estimate the NO_x source strength from lightning:

(1) Multiply the frequency of lightning flashes by the energy dissipated per flash and the NO production per unit of energy dissipated; or
(2) Relate NO_x production to NO_3^- deposition in remote areas where lightning-produced NO_x is thought to be the dominant NO_3^- precursor.

Method 1 yields an annual NO_x production of approximately 1.2 Tg for North America (Placet et al., 1991). The deposition-based estimate (Method 2) gives a somewhat larger value of 1.7 Tg/year (Placet et al., 1991). The NAPAP inventory included lightning-produced NO_x on a gridded 10° × 10° latitude-longitude scale. Most of the continental United States fits within 30° to 50° N latitude and 80° to 120° W longitude. The estimated annual lightning-produced NO_x for this region (continental United States) is about 1.0 Tg. Roughly 60% (0.6 Tg) of this NO_x is generated over the southern tier of states (30° to 40° N latitude; 80° to 120° W longitude).

Soils. Both nitrifying and denitrifying organisms in the soil can produce NO_x. The relative importance of these two pathways is probably highly variable from biome to biome. Nitric oxide is the principal NO_x species emitted from soils, with emission rates depending mainly on fertilization levels and soil temperature. Several reports have noted a large increase in NO_x emissions from agricultural soils treated with NO_3^--containing fertilizers (Johansson and Granat, 1984; Kaplan et al., 1988; Johansson, 1984). Measurements of soil NO_x emissions have established that the relationship with temperature is exponential,

consisting of approximately a twofold increase for each 10 °C rise in temperature (Williams et al., 1992; Valente and Thornton, 1993).

Inventorying soil NO_x emissions is difficult because of the large temporal and spatial variability in emissions. The existing inventories have been developed using emission algorithms that are functions of soil temperature and land-use type. Two broad, land-use categories—natural and agricultural—have been assigned. The natural soils are broken down into biome types, and the agricultural soils subdivided according to fertilizer applications. The highest biogenic NO emissions are in corn-growing regions of the midwest (Nebraska, Iowa, and Illinois) during summer months. Of the total U.S. biogenic emissions of NO from soils, 85% occur during the spring and summer months.

Table 3-10 provides a summary of the annual soil NO_x emissions from the 10 U.S. Environmental Protection Agency regions. Approximately 60% of this NO_x is emitted in Regions V, VII, and VIII (see Figure 3-19), which contain the central U.S. corn belt. The total estimate for U.S. soil emissions is 1.2 Tg.

Table 3-10. Annual Nitrogen Oxides Emissions from Soils by U.S. Environmental Protection Agency Region[a]

U.S. Environmental Protection Agency Region	NO_x Emissions (Tg)
I, II, and III	0.05
IV	0.11
V	0.26
VI	0.18
VII	0.27
VIII	0.21
IX	0.04
X	0.01
Total	1.20[b]

[a]See Appendix A for abbreviations and acronyms.
[b]Values do not sum to total due to independent rounding.

Source: Placet et al. (1991).

Uncertainty in Estimates of Natural Nitrogen Oxides Emissions

As previously indicated, inventorying NO_x produced from lightning requires multiplying the number of flashes by average energy factors. No attempt has been made to assign confidence limits to these variables. A measure of the uncertainty associated with lightning-produced NO_x is provided, however, by comparing emission estimates generated independently. Two estimates of the amount of lightning-generated, summertime NO_x in the southeastern United States (2.4 and 8.5×10^{-2} Tg) varied by approximately a factor of 4 (Placet et al., 1991).

Sources of uncertainty when inventorying NO_x emissions from soils include: land-use assignments, soil temperature, and emission algorithm development. Confidence levels assigned to categories 1 and 2 are about ±50%. The emission algorithm is developed from field measurements of NO_x emission rates versus temperature for various land-use categories. Measurement accuracy is approximately ±30%. However, because of the natural variability of NO_x emissions within a specific soil category, uncertainty in the exponential relationship that relates emission rate to temperature is estimated to be in the range of a factor of 2 to 4.

Comparison of Emissions from Manmade and Natural Sources

On an annual basis, natural sources (lightning and soils) contribute approximately 2.2 Tg of NO_x to the troposphere over the United States. This compares to the 1990 anthropogenic emission estimate of 19.4 Tg. Annual NO_x emissions from soils (1.2 Tg) are about 6% of the manmade emissions in the United States. This percentage increases to about 14% when the comparison includes only the summer months of July, August, and September. Even larger biogenic contributions can occur in certain regions of the United States. For example, it is estimated that biogenic NO_x emissions from soils account for about 19% of summertime NO_x emissions in Tennessee (Valente and Thornton, 1993) and actually exceed emissions from manmade sources during the summer months in the states of Nebraska and South Dakota (Williams et al., 1992).

3.4.1.3 Volatile Organic Compounds

Manmade Emission Sources

Volatile organic compounds are emitted into the atmosphere by evaporative and combustion processes. Many hundreds of different organic species are released from a large number of source types. The species commonly associated with atmospheric O_3 production contain from 2 to about 12 carbon atoms. They can be true hydrocarbons, which possess only carbon and hydrogen atoms (e.g., alkanes, alkenes, aromatics), or substituted hydrocarbons that contain a functional group such as alcohol, ether, carbonyl, ester, or halogens. The emissions of methane have been ignored because of their largely natural origin and the fact that the importance of methane is limited primarily to global scale processes. In addition, the atmospheric oxidation rate of methane is very slow compared to the higher molecular weight organics.

In 1991, the total U.S. emissions of VOCs was estimated to be 21.0 Tg (U.S. Environmental Protection Agency, 1993b). The two largest source categories were industrial processes (10.0 Tg) and transportation (7.9 Tg). Lesser contributions were attributed to waste disposal and recycling (2.0 Tg), stationary source fuel combustion (0.7 Tg), and miscellaneous area sources (0.5 Tg). Table 3-11 provides a more detailed breakdown of VOC source contributions. Within the industrial category, solvent utilization, petroleum product storage and transfer, and chemical manufacturing are the major contributors. Volatile organic compounds released from highway vehicles account for almost 75% of the transportation-related emissions.

Speciated hydrocarbon emissions from manmade sources were reported in the 1985 NAPAP Emissions Inventory. Emissions of each main hydrocarbon family exceeded 1 Tg. Alkanes comprised about 33%, aromatics 19%, and alkenes 11% of anthropogenic VOC emissions in the 1985 inventory (Placet et al., 1991). None of the major oxygenated

Table 3-11. Estimated 1991 Emissions of Volatile Organic Compounds from Manmade Sources in the United States

Source Category	Emissions (Tg)	
Transportation		7.87
Highway vehicles	6.00	
Off-highway vehicles	1.87	
Stationary fuel combustion		0.68
Electric utilities	0.03	
Industrial	0.26	
Other	0.39	
Industrial processes		9.97
Chemical manufacture	1.61	
Petroleum and related industries	0.68	
Solvent utilization	5.50	
Petroleum product storage and transport	1.69	
Other	0.49	
Waste disposal and recycling		2.01
Miscellaneous		0.51
Total all sources		21.04

Source: U.S. Environmental Protection Agency (1993b).

hydrocarbon groups (e.g., carbonyls, organic acids, phenols) listed in the speciated inventory exceeded 1 Tg. The carbonyl group, which included formaldehyde, higher aldehydes, acetone, and higher ketones, was the largest contributor of oxygenated hydrocarbons at 0.73 Tg.

Seasonal variations are available for the 1993 anthropogenic VOC emissions from 14 source categories in the United States (U.S. Environmental Protection Agency, 1994). Very few seasonal variations occur for categories contributing approximately 85% of the total annual VOC emissions. The only category of VOC emissions that showed significant seasonal variation was off-highway sources, which comprises 13% of the total annual VOC emissions. These off-highway sources contribute 31% of their VOC emissions in summer and 19% in winter. An earlier inventory for 1985 (U.S. Environmental Protection Agency, 1989), which considered total point and area anthropogenic VOC emissions, indicated that very little variation in VOC emissions occurred between the winter, spring, summer, and fall seasons. The contribution of these VOC emissions also were shown to vary seasonally by region of the United States.

Trends in Emissions

Emissions of nonmethane VOCs peaked in the early 1970s and have decreased continually since then. Emissions of VOCs increased from 15.5 Tg in 1940 to 27.4 Tg in

1970 and now are estimated to be back down to approximately the same level as in 1940 (U.S. Environmental Protection Agency, 1992a). Figure 3-22 illustrates these changes at 10-year intervals from 1940 to 1990. Until 1970, highway vehicles were the major source of VOC emissions. As automobiles have been equipped with more and better emission controls, however, emissions from the transportation sector have dropped below those from industrial processes, the category that is now the leading contributor of VOC emissions to the atmosphere. Transportation, industrial processes, and the miscellaneous burning and solvent-use categories have accounted for 83 to 93% of VOC emissions over the past 50 years. Figure 3-23 shows the emission trends for these three categories. The transportation-related emissions of VOCs are currently estimated to be at about the same level as in 1940. Industrial process VOC emissions nearly tripled between 1940 and 1980, followed by a small decline in more recent years. The miscellaneous category exhibited a decrease in emissions from 4.5 Tg in 1940 to a 1990 level estimated at 2.8 Tg/year.

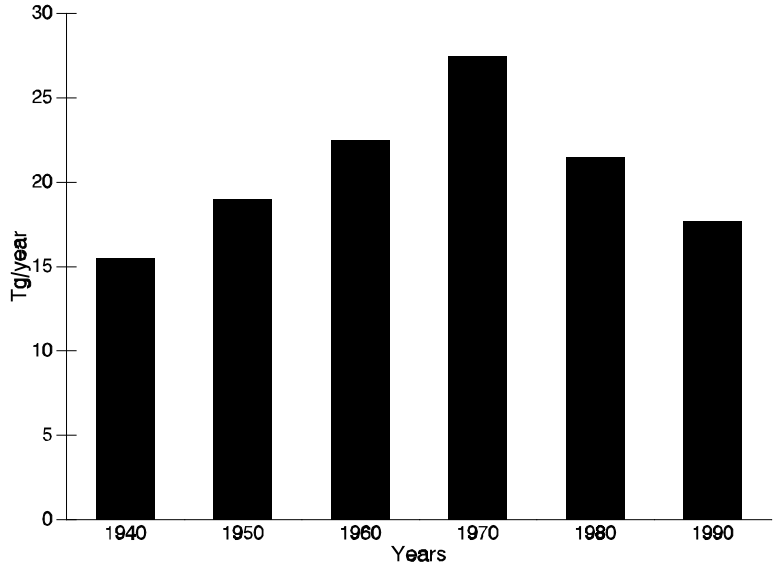

Figure 3-22. Changes in emissions of volatile organic compounds from major manmade sources in the United States, 10-year intervals, 1940 through 1990.

Source: U.S. Environmental Protection Agency (1992a).

Trends for the dominant VOC emissions categories from 1987 through 1991 are shown in Table 3-12. Projections for the year 2000 forecast a 62% reduction in VOC emissions from highway vehicles compared to 1990 levels. The major reduction in the transportation area will contribute to a predicted overall 25% decrease in total national VOC emissions between 1990 and 2000 (U.S. Environmental Protection Agency, 1992a).

Uncertainty in Estimates of Emissions from Manmade Sources

It has proven difficult to determine the accuracy of VOC emission estimates. Within an area source such as an oil refinery, emission factors and activity levels are

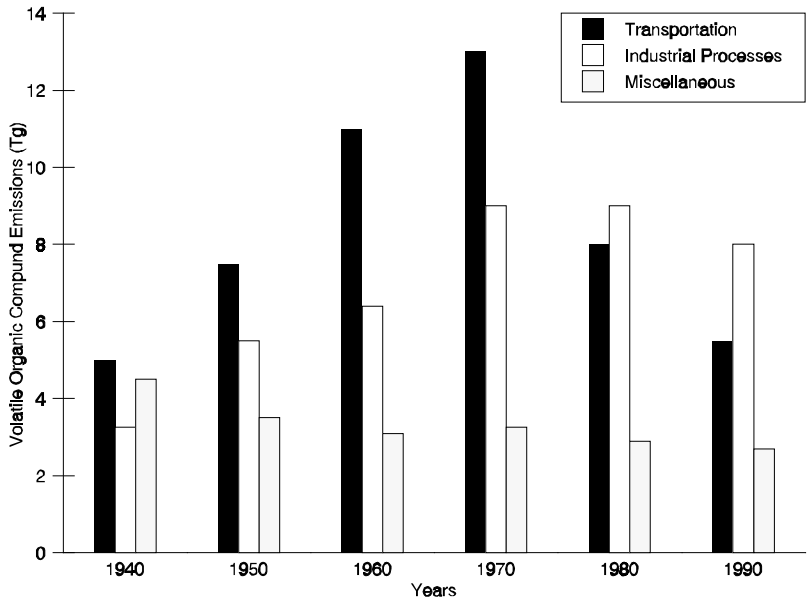

Figure 3-23. Changes in emissions of volatile organic compounds from major manmade sources, 1940 through 1990.[a]

[a]The values for 1990 do not agree with those in Table 3-12 because different models were employed for deriving the short- and long-term trends.

Source: U.S. Environmental Protection Agency (1992a).

Table 3-12. Recent Trends in Emissions of Volatile Organic Compounds from Major Categories of Manmade Sources (Tg)

Year	Transportation	Industrial Processes	Waste Disposal and Recycling
1991	7.87	7.86	2.01
1990[a]	8.07	9.96	2.05
1989	8.26	9.92	2.08
1988	9.15	10.00	2.10
1987	9.29	9.65	2.05

[a]The values for 1990 do not agree with those in Figure 3-23 because different models were employed for deriving the short- and long-term trends.

Source: U.S. Environmental Protection Agency (1993b).

assigned for thousands of individual sources (e.g., valves, flanges, meters, processes), and emission estimates for each of these sources are summed to produce the emissions total. Because it would be impractical to determine an emission factor for each of these sources within a refinery individually, average emission factors for the various source categories are utilized. This can lead to substantial error if emissions from the individual sources deviate from the assigned average factor. Even more troublesome are area sources that include a large evaporative emissions component. These sources are dependent on environmental factors such as temperature, which add to the difficulty in establishing reliable emission estimates. Such sources fall into a miscellaneous solvent evaporation category that includes emissions from processes such as dry cleaning, degreasing, printing, automobile body repair, furniture manufacture, and motor vehicle manufacture.

Assigning accurate VOC emission estimates to the mobile source category has proven troublesome, as well. Models are used that incorporate numerous input parameters, each of which has some degree of uncertainty. For example, activity models are employed to characterize the mobile source fleet. This includes the number of vehicles in various categories (e.g., gasoline-fueled, diesel-fueled, catalyst-equipped, non-catalyst-equipped, etc.), miles accumulated per year for each type of vehicle, and ages of the vehicles. Vehicle registration statistics are employed for category assignment. Errors can arise because registration data are not always up to date, and unregistered vehicles are completely omitted. Military vehicles, foreign-owned automobiles, and old "junkers" that are on the highways but not registered are included in the inventorying process. The activity models assume that vehicles of the same age accumulate mileage at the same rate. This is most likely not correct; there is a need to assess the uncertainty in this assumption through a systematic collection of vehicle type, age, and mileage accumulation statistics.

Experiments carried out in tunnels have looked at the relationship between measured VOC emission factors and those derived from automotive emission models. In a study designed to verify automotive emission inventories for the South Coast Air Basin, measurements in the Van Nuys Tunnel indicated that automotive VOC emissions were a factor of 4 larger than predicted using emission models (Pierson et al., 1990). Results from two tunnel studies conducted in 1992 (Robinson et al., 1996) show much better agreement between VOC measurements and model predictions than those obtained in the Van Nuys Tunnel. Comparisons were made for the Tuscarora Tunnel on the Pennsylvania Turnpike in south-central Pennsylvania and at the Fort McHenry Tunnel under Baltimore Harbor. For Tuscarora, MOBILE4.1 gives 131% of the average measured VOC values and MOBILE5 gives 216% of the average measured VOCs. For Fort McHenry, MOBILE4.1 gives 53% of the average measured VOC values and MOBILE5 gives 81% of the average measured VOCs. Somewhat better agreement also was obtained from the Van Nuys Tunnel data when the updated California emission model EMFACTEP was used (Robinson et al., 1996). At the Cassier Tunnel in Vancouver, Canada, agreement within ±30% was obtained between the VOC measurements and the Canadian version of the MOBILE models (Gertler et al., 1994). The 1993 results from the Caldecott Tunnel in the San Francisco, CA, area show deviations between VOC measurements and model predictions similar to those obtained in the Van Nuys Tunnel, possibly because of similar urban/local fleets. Differences in test results between the newer tunnel studies and those obtained in the early Van Nuys Tunnel study are likely due to the better condition of the vehicles in the newer studies and the lack of power enrichment or other transients because of the steady-speed driving. However, it is important to appreciate that results from tunnel measurements do not necessarily predict equivalency of VOC

measurements with model predictions under highly transient urban/local driving and fleet conditions.

Recent developments in remote sensing have permitted more accurate measurement of hydrocarbon exhaust emissions from on-road vehicles (Stedman et al., 1991). These studies have demonstrated a highly skewed distribution, with the majority of VOC emissions coming from about 20% of the automobiles. Emission factors developed from laboratory dynamometer testing most likely do not properly account for the high-emitting vehicle contribution (Pitchford and Johnson, 1993). In many cases, these high emitters are older cars that are poorly maintained. In order to reduce this source of uncertainty, it may be necessary to reassess the life spans assigned to vehicles. Vehicles manufactured more than 25 years prior to 1993 are not included in the inventory. However, these older vehicles are likely to be high emitters, and, if they are underrepresented in the model, emissions will be underestimated. Activity models provide data in terms of national averages. This can contribute to inaccuracies in emissions estimates if a particular region varies from the national average in terms of vehicle types, age, or VMT.

Ambient measurements of VOCs and NO_x have been employed in order to better define uncertainty levels in VOC inventories. Some of the earliest work was carried out in the Atlanta area in the 1980s. Using a simple model and measured ambient VOC and NO_x concentrations, it was shown that ambient NO_x levels were consistent with the urban NO_x emission estimates. However, measured ambient VOC concentrations were as much as a factor of 6 greater than predicted (Westberg and Lamb, 1985). Improvements in mobile source emission models have resulted in somewhat higher emission estimates, so that the discrepancy between model estimates and ambient data has been reduced to about a factor of 2.5 (Fujita et al., 1992; Cadle et al., 1993). It is clear that the relationship between emission inventories and ambient concentrations of NO_x and VOCs warrants further study. In addition to improving the mobile source emission inventories, it will be necessary to place uncertainty bounds on stationary source inventories. Whether stationary source emissions of VOCs are underpredicted using current emission inventory methodology is not known (Finlayson-Pitts and Pitts, Jr., 1993).

Biogenic Emissions

Vegetation emits significant quantities of reactive VOCs into the atmosphere. Many of these biogenic VOCs may contribute to O_3 production in urban (Chameides et al., 1988) and rural (Trainer et al., 1987) environments. The VOC emissions of primary interest are isoprene and the monoterpenes (e.g., α-pinene, β-pinene, myrcene, limonene, etc.), which are hydrocarbons. Recent field measurements have shown that a variety of oxygenated organics also are emitted from plants (Winer et al., 1992). A thorough discussion of biogenic emissions and their implication for atmospheric chemistry has been published recently by Fehsenfeld et al. (1992), who reviewed the techniques used to measure VOC emissions from vegetation, laboratory emissions studies that have been used to relate emission rates to temperature and light intensity, development of emission models, and the use of emission models in the preparation of emission inventories.

Since the late 1970s, a number of regional and national biogenic emission inventories have been reported (Zimmerman, 1979; Winer et al., 1983; Lamb et al., 1985, 1987, 1993). These inventories are based on algorithms that relate VOC emissions from a particular vegetation class to ambient temperature, land-use, and, in the case of isoprene, photosynthetically active radiation. Most biogenic VOC emissions from vegetation increase

exponentially with temperature. Isoprene emissions are light-dependent, being minimal at night and increasing with solar intensity during the day. Deciduous vegetation is the dominant source of isoprene; whereas coniferous trees emit primarily monoterpenes. Other things being equal, isoprene is emitted at a much higher rate than the monoterpenes. For example, in a southern forest of mixed pine and hardwoods, the isoprene emission rate from an oak tree is about 10 times larger than the flux of α-pinene from an adjacent loblolly pine during the midday period.

The most recent biogenic VOC emissions estimate for the United States totals 29 Tg/year (Lamb et al., 1993). This estimate includes 5.9 Tg isoprene, 4.4 Tg α-pinene, 6.5 Tg other monoterpenes, and 12.3 Tg other VOCs. Table 3-13 provides a summary of the contributions from the various vegetation categories based on an inventory of monthly statewide data for eight land-cover types. In preparing this inventory, algorithms were developed that related VOC emissions to temperature and light for each of the biomass categories shown in the table. On a national scale, coniferous forests are the largest vegetative contributor because of their extensive land coverage. The category "Other VOCs" is the dominant biogenic hydrocarbon contributor to the national total. From the standpoint of inventory accuracy, this is somewhat unfortunate because the identities of most of the "Other VOCs" are uncertain. This classification has carried over from the extensive field-measurement program conducted by Zimmerman (1979) and coworkers in the mid-1970s. The category "Other VOCs", includes peaks that showed up in sample chromatograms at retention times that could not be matched to known hydrocarbons. It is likely that if the Zimmerman study were repeated today, most of the species making up this "Other VOCs" category could be identified. Recent field studies have made use of GC/MS techniques that were not available to Zimmerman in the 1970s.

Biogenic emissions, because of their dependence on temperature and vegetational growth, vary by season. In addition, the southern tier of states is expected to produce more biogenic emissions than those in the north because of higher average temperatures. Table 3-14 shows a spatial and temporal breakdown of U.S. biogenic emissions. Summertime emissions comprise 16.7 of the 29.1 Tg (or 57%) of the annual totals in all regions. The EPA Regions IV and VI in the southeastern and southcentral United States, respectively, have the highest summertime and annual biogenic VOC emission rates. Region IV contributes 16% of the summertime and 18% of the annual biogenic VOC emissions in the United States, whereas Region VI contributes 21% of the summertime and 23% of the annual biogenic emissions in the United States. Compared to Regions IV and VI, regions to the north have more rapid increases in biogenic VOC emissions in the spring and more rapid decreases in biogenic VOC emissions in the fall.

Uncertainty in Estimates of Biogenic Emissions

Sources of error in the biogenic inventorying process arise from uncertainties in emission measurements, determination of biomass densities, land-use characterization, and measurement of light intensity and temperature. Within each of these categories, the error is relatively small. However, when emission measurements are combined with temperature or light intensity, or both, into a single algorithm, the uncertainty increases greatly. This results from the fact that temperature and light are only surrogates for the real physiological processes that control biogenic emissions. Emission rate and ambient temperature can be highly correlated for data collected from one tree branch over a 24-h period; but, when these data are combined with measurements from other branches and other trees the correlation is

Table 3-13. Annual Biogenic Hydrocarbon Emission Inventory for the United States (Tg)[a]

	Land Use								
Compound	Oak Forests	Other Deciduous Forests	Coniferous Forests	Scrub-lands	Grass-lands	Crop-lands	Inland Waters	Urban Areas	U.S. Total
Isoprene	2.31	1.01	0.61	1.17	0.49	0.2	0.02	0.08	5.9
α-pinene	0.19	0.23	2.07	0.78	0.13	0.85	0.06	0.04	4.4
Other terpenes	0.41	0.44	3.08	1.41	0.24	0.81	0.06	0.06	6.5
Other VOCs	1.12	0.88	2.72	2.49	0.45	4.51	0.07	0.08	12.3
Total	4.03	2.56	8.48	5.85	1.31	6.37	0.21	0.26	29.1
Percent of Total	13.9	8.8	29.2	20.1	4.5	21.9	0.7	0.9	

[a]See Appendix A for abbreviations and acronyms.

Source: Lamb et al. (1993).

Table 3-14. Annual Biogenic Hydrocarbon Emission Inventory by Month and by U.S. Environmental Protection Agency Region for United States Emissions (Tg)

	U.S. Environmental Protection Agency Region									
Month	III	IV	V	VI	VII	VIII	IX	X	Total	Percent of Total
1	0.018	0.092	0.004	0.084	0.007	0.022	0.060	0.043	0.3	1.1
2	0.017	0.139	0.004	0.123	0.007	0.020	0.054	0.039	0.4	1.4
3	0.071	0.428	0.067	0.519	0.078	0.108	0.113	0.102	1.5	5.1
4	0.169	0.460	0.189	0.567	0.211	0.303	0.320	0.202	2.4	8.3
5	0.206	0.475	0.240	0.586	0.226	0.362	0.331	0.208	2.6	9.1
6	0.427	0.874	0.550	1.146	0.508	0.809	0.710	0.424	5.5	18.7
7	0.441	0.903	0.568	1.184	0.524	0.836	0.734	0.438	5.6	19.3
8	0.439	0.903	0.568	1.184	0.524	0.820	0.734	0.438	5.6	19.3
9	0.123	0.461	0.137	0.561	0.136	0.280	0.357	0.212	2.3	7.8
10	0.069	0.286	0.066	0.394	0.026	0.290	0.369	0.219	1.7	5.9
11	0.066	0.162	0.063	0.174	0.025	0.110	0.130	0.109	0.8	2.9
12	0.018	0.080	0.004	0.073	0.007	0.022	0.060	0.043	0.3	1.1
Total	2.1	5.3	2.5	6.6	2.3	4.0	4.0	2.5	29.1	

Source: Lamb et al. (1993).

not nearly as good. The uncertainty associated with the algorithms used to generate the U.S. inventory described previously is estimated to be a factor of 3 (Lamb et al., 1987). Because other sources of error in the inventorying process are much smaller, a factor of 3 is the current best estimate of the overall uncertainty associated with biogenic VOC inventories. However, this may be a lower limit if it is shown that oxygenated species are emitted in significant quantities by vegetation. Emission measurement methods employed in the past have not been adequate for quantifying polar, oxygenated organics.

Comparison of Manmade and Biogenic Emissions

The most recent anthropogenic and biogenic VOC emissions estimates for the United States indicate that natural emissions (29 Tg) exceed manmade emissions (23 Tg). During the summer months in the United States, anthropogenic emissions constitute 25% of the annual anthropogenic VOC emissions, whereas biogenic emissions constitute 57% of the annual biogenic emissions. On a teragram basis, anthropogenic VOC emissions during the summer contribute 0.25×23 Tg = 5.75 Tg, whereas summer biogenic VOC emissions contribute 0.57×29 Tg = 16.5 Tg. Therefore, on a national basis, the ratio of biogenic to anthropogenic VOC emissions is approximately 2.9 for the United States. However, this ratio varies with region in the summer months. These calculations depend on the assumption that regional summertime anthropogenic VOC emissions are one-quarter of the annual VOC emissions. With this assumption, the ratios of biogenic to anthropogenic VOC emissions for three selected regions are as follows: 2.2 for Region IV, 1.6 for Region V, and 3.2 for Region VI (Lamb et al., 1993; U.S. Environmental Protection Agency, 1994). However, in a recent National Research Council review (1991), it was concluded that emissions from manmade sources are currently underestimated by a significant amount (60 to 80%). Because uncertainty in both biogenic and anthropogenic VOC emission inventories is large, it is not possible to establish whether the contribution of emissions from natural or manmade sources of VOCs is larger.

3.4.1.4 Relationship of Summertime Precursor Emissions and Ozone Production

Peak O_3 levels are recorded in most regions of the country during the months of June, July, and August. From the foregoing discussion, it is obvious that natural emissions of NO_x and VOCs peak during this same time frame. Biogenic emissions are very dependent on temperature; and, as ambient temperatures rise during the summer months, NO_x and VOC emissions reach a maximum. Figure 3-24 clearly demonstrates this for biogenic VOC emissions, and a plot of monthly biogenic NO_x emissions would show a similar pattern. Well over 50% of biogenic NO_x and VOC emissions occur during the period of maximum photochemical activity.

Seasonal changes in anthropogenic emissions of NO_x are believed to be relatively small. The transportation sector produces slightly less NO_x during the warmer months, but there is probably a small increase from the stationary source category because of higher summertime power demands. Because these are the major U.S. sources of NO_x and changes in seasonal emissions tend to offset each other, there is no reason to expect that NO_x emissions will vary significantly by season on the national level. Evaporative emissions of VOCs are enhanced during the warm summer months. Because evaporation is an important component of anthropogenic VOC emissions, there is a summertime increase. In 1993, U.S. VOC emissions during June, July, and August were estimated to exceed annual monthly average VOC emissions by about 17% (U.S. Environmental Protection Agency, 1994). The